

Effect of ion pairs in fast-light bandwidth in high-concentration erbium-doped fibers

Oscar G. Calderon,* Sonia Melle, Francisco Arrieta-Yañez, M. A. Anton, and F. Carreño

*Escuela Universitaria de Óptica, Universidad Complutense de Madrid, C/ Arcos de Jalón s/n,
28037 Madrid, Spain*

*Corresponding author: oscargc@opt.ucm.es

Received May 30, 2008; accepted June 25, 2008;
posted July 7, 2008 (Doc. ID 96872); published September 17, 2008

The effect of ion pairs in high-concentration erbium-doped fibers on slow- and fast-light propagation enabled by coherent population oscillations at room temperature has been experimentally investigated. We find that an increase of the erbium ion concentration increases the fractional advancement although it degrades the bandwidth of the modulated signals that propagate at superluminal velocities due to the presence of ion pairs in the fiber. © 2008 Optical Society of America

OCIS codes: 190.4370, 270.1670, 060.2410.

1. INTRODUCTION

Controlling the speed of light in optical fibers at room temperature is a task that has received recent attention since these devices would be compatible with fiber-optic communication systems and represent a great step towards the development of all-optical signal processing devices. Song *et al.* [1] and Okawachi *et al.* [2] observed slow and fast light in optical fibers for the first time by using stimulated Brillouin scattering (SBS). This method consists of the interaction of two propagating waves, a pump wave and a Stokes wave, which generates an acoustic wave at the difference frequency of the pump and Stokes fields. The slow-light resonance can be placed at the desired frequency by changing the pump wavelength. A related process, stimulated Raman scattering (SRS), has also been used in an optical fiber to demonstrate an ultrafast all-optical controllable delay [3].

More recently, a modification of group velocity in an erbium-doped fiber (EDF) has been reported by Schweinsberg *et al.* [4] based on coherent population oscillation (CPO). The first experiments based on this coherent process were done by Bigelow *et al.* in different solid-state materials at room temperature [5,6]. This process is easily achieved in a two-level system that interacts with an amplitude-modulated signal. The population of the ground state of the medium will be induced to oscillate at the modulation frequency. This oscillation creates a narrow hole in the absorption or gain spectrum, whose linewidth is proportional to the inverse of the relaxation lifetime of the excited level [7]. Schweinsberg *et al.* [4] reported a change from subluminal to superluminal propagation upon increasing pump power in a 13 m long EDF with Er ion density of $1.78 \times 10^{24} \text{ m}^{-3}$ [90 parts per million (ppm)] where an amplitude-modulated 1550 nm signal copropagates with a 980 nm pump beam. By using the same experimental system, fast-light pulse propagation has been studied in more detail in [8,9].

Many applications concerning EDF amplifiers, such as

high-speed optical telecommunications, require one to minimize the fiber length to construct compact and integrated devices. Then, a high ion doping level is needed to have a good pump light absorption. However, experiments have shown deleterious effects of ion pairs via inhomogeneous upconversion processes on the output performance of high-concentration EDF amplifiers [10,11]. Sanchez *et al.* [10] showed that erbium ion pairs can behave as a saturable absorber and lead to self-pulsing operation in EDF lasers when the fraction of paired ions reaches a sufficient level. Moreover, Wagener *et al.* [11] reported that as the dopant level increases, the laser threshold increases and the slope efficiency decreases. They also characterized the increase of the percentage of pairs in the fiber with the concentration. Several theoretical models, including ion pairs interaction, have been developed to explain these phenomena [12,13].

Recently, the effect of ion density on slow-light propagation enabled by CPO has been experimentally investigated for highly doped erbium fibers [14,15]. It was found that a high ion concentration can increase the fractional delay up to a saturation value. Furthermore, by pumping these highly doped erbium fibers, a propagation-induced superluminal to subluminal transition has been observed [16]. As a consequence, solely upon an increase of the modulation frequency a switch from delay to advancement occurs. Here, we analyze in detail the role of the ion pairs in the slow- and fast-light propagation in highly doped erbium fibers. The theoretical model used to study CPO in highly doped erbium fibers is described in Section 2 and is based on [13]. The experimental setup and results are presented in Section 3 with a discussion about the estimation of the number of ion pairs in Subsection 3.A. The final conclusions are given in Section 4.

2. MODEL

Previous works have shown that upconversion processes via interparticle interactions are the main cause of EDF

gain degradation. In this process one initially excited (${}^4I_{13/2}$) erbium ion (donor) donates its energy to a neighbor excited erbium ion (acceptor), producing one upconverted ion and one ground-state ion (${}^4I_{15/2}$). The upconverted ion then relaxes rapidly to the initial excited state ${}^4I_{13/2}$. As a result of this interaction one excited ion is lost. There are two different kinds of upconversion processes. The first one is the homogeneous upconversion (HUC) in which the ions are uniformly distributed and the energy transfers from one ion to its neighbor with a characteristic time of a few milliseconds. The second one is the inhomogeneous upconversion, or pair-induced quenching (PIQ), in which the ions are not uniformly distributed and the energy transfer happens between two adjacent excited paired ions with a characteristic time of a few microsecond. Therefore, the PIQ is the dominant upconversion process in high-concentration EDFs.

Following the model developed by Li *et al.* [13] to explain the effect of ion pairs on the output performance of EDF lasers, we divided the erbium ions into two groups: isolated ions with an excited-state lifetime close to 10 ms and paired ions with a very fast decay of the pair excited-state ${}^4I_{13/2}$ (close to microseconds). By assuming a rapid decay from the upper pump state (${}^4I_{11/2}$), the isolated ions can be described by a two-level system, the ground state ${}^4I_{15/2}$ and the upper laser level ${}^4I_{13/2}$ with population densities N_1 and N_2 , respectively [see Fig. 1(a)]. Then, the rate equation for N_1 is

$$\frac{dN_1}{dt} = \frac{\rho(1-2k) - N_1}{\tau} + \frac{P_s \sigma_{12}}{\hbar \omega_s A_s} [\beta_s \rho(1-2k) - (1 + \beta_s) N_1] - \frac{P_p \sigma_{13}}{\hbar \omega_p A_p} N_1, \quad (1)$$

where t is the time variable and $\tau=10.5$ ms is the lifetime of the metastable state ${}^4I_{13/2}$. P_s and P_p are the signal and pump powers, respectively. σ_{21} and σ_{12} are the emission and absorption cross sections, respectively, at the signal frequency ω_s . A_s is the signal mode area. The ratio between the signal cross sections is $\beta_s = \sigma_{21}/\sigma_{12}$. σ_{13} is the absorption cross section at the pump frequency ω_p and A_p is the pump mode area. k is the fraction of ion pairs in the total ion concentration ρ , then $N_1 + N_2 = \rho(1-2k)$. The ion pairs can be described as a three-level system: the ground state (${}^4I_{15/2}$, ${}^4I_{15/2}$), the intermediate level (${}^4I_{15/2}$, ${}^4I_{13/2}$), and the upper level (${}^4I_{15/2}$, ${}^4I_{13/2}$) with population densities N_{11} , N_{12} , and N_{22} , respectively [see Fig. 1(b)]. For the

sake of simplicity, and due to the fast decay of the upper level, we consider only the two lower levels, i.e., $N_{11} + N_{12} \approx \rho k$. Then, the rate equation for N_{11} is

$$\frac{dN_{11}}{dt} = \frac{\rho k - N_{11}}{\tau} + \frac{P_s \sigma_{12}}{\hbar \omega_s A_s} [\beta_s \rho k - (1 + \beta_s) N_{11}] - \frac{P_p \sigma_{13}}{\hbar \omega_p A_p} N_{11}. \quad (2)$$

The propagation equations of the signal power P_s and the pump power P_p are

$$\frac{dP_s}{dz} = \sigma_{12} \eta_s [\beta_s \rho(1-2k) - (1 + \beta_s) N_1 + (\beta_s - 1) \rho k - \beta_s N_{11}] P_s, \quad (3)$$

$$\frac{dP_p}{dz} = -\sigma_{13} \eta_p (N_1 + \rho k) P_p, \quad (4)$$

where $\eta_s = A_c/A_s$ ($\eta_p = A_c/A_p$) is the ratio between the fiber core area A_c and the signal A_s (pump A_p) mode area. When we modulate the signal power as $P_s = P_0 + P_m \cos(2\pi f_m t)$ (where P_0 is the average signal power, P_m is the modulation amplitude, and f_m is the modulation frequency), the ground-state population of both isolated and paired ions will be forced to oscillate with the same frequency as $N_1 = N_{1st} + N_{1c} \cos(2\pi f_m t) + N_{1s} \sin(2\pi f_m t)$ and $N_{11} = N_{11st} + N_{11c} \cos(2\pi f_m t) + N_{11s} \sin(2\pi f_m t)$, respectively, where the steady-state populations and the amplitude of the populations oscillations can be obtained from Eqs. (1) and (2),

$$N_{1st} = \frac{\rho(1-2k)}{w_c} \left(1 + \frac{\beta_s}{1 + \beta_s} \hat{P}_0 \right), \quad (5)$$

$$N_{1c} = \frac{w_c}{w_c^2 + (2\pi f_m \tau)^2} \left(\frac{\beta_s \rho(1-2k)}{1 + \beta_s} - N_{1st} \right) \hat{P}_m, \quad (6)$$

$$N_{1s} = \frac{2\pi f_m \tau}{w_c^2 + (2\pi f_m \tau)^2} \left(\frac{\beta_s \rho(1-2k)}{1 + \beta_s} - N_{1st} \right) \hat{P}_m, \quad (7)$$

$$N_{11st} = \frac{\rho k}{w_c} \left(1 + \frac{\beta_s}{1 + \beta_s} \hat{P}_0 \right), \quad (8)$$

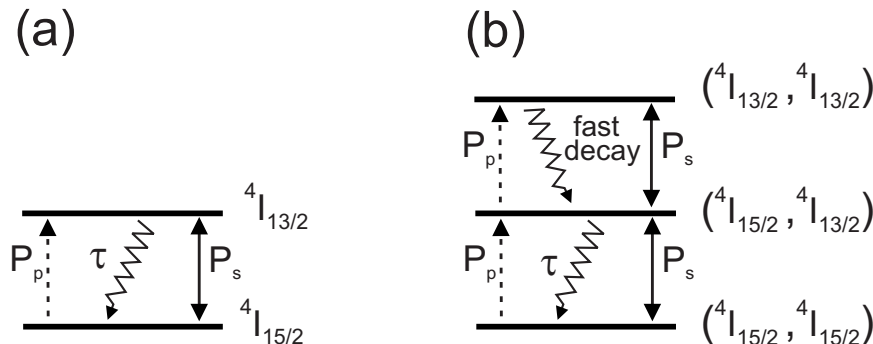


Fig. 1. (a) Two-level system for isolated Er ions and (b) the three-level system for Er ion pairs.

$$N_{11c} = \frac{w_c}{w_c^2 + (2\pi f_m \tau)^2} \left(\frac{\beta_s \rho k}{1 + \beta_s} - N_{11st} \right) \hat{P}_m, \quad (9)$$

$$N_{11s} = \frac{2\pi f_m \tau}{w_c^2 + (2\pi f_m \tau)^2} \left(\frac{\beta_s \rho k}{1 + \beta_s} - N_{11st} \right) \hat{P}_m, \quad (10)$$

where $\hat{P}_0 \equiv P_0/P_{0sat}$ ($\hat{P}_m \equiv P_m/P_{0sat}$) is the ratio of P_0 (P_m) to the signal saturation power $P_{0sat} = \hbar \omega_s A_s / (\tau(\sigma_{21} + \sigma_{12}))$. $\hat{P}_p \equiv P_p/P_{psat}$ is the ratio of P_p to the pump saturation power $P_{psat} = \hbar \omega_p A_p / (\tau \sigma_{13})$. $w_c = 1 + \hat{P}_0 + \hat{P}_p$ is a dimensionless frequency that determines the width of the transparency hole created in the absorption or gain spectrum by means of CPO. Note that this magnitude roughly measures the maximum modulation bandwidth that can experience the full slow- or fast-light effect [17] and is power broadened.

Finally, we can obtain the propagation equations for the average powers and the phase shift experienced by the periodic part of the signal ϕ , which measures the time delay $t_d = \phi/f_m$:

$$\frac{d\hat{P}_0}{dz'} = -\frac{\alpha_s}{\rho} \hat{P}_0 [(1 + \beta_s)N_{1st} - \beta_s \rho (1 - 2k) + \rho k (1 - \beta_s) + \beta_s N_{11st}], \quad (11)$$

$$\frac{d\hat{P}_p}{dz'} = -\frac{\alpha_p}{\rho} \hat{P}_p (N_{1st} + \rho k), \quad (12)$$

$$\frac{d\phi}{dz'} = \frac{\alpha_s}{\rho} \hat{P}_0 \left[(1 + \beta_s) \left(\frac{N_{1s}}{\hat{P}_m} \right) + \beta_s \left(\frac{N_{11s}}{\hat{P}_m} \right) \right], \quad (13)$$

where the distance $z' = z/L$ has been normalized with the fiber length L . $\alpha_s = L\sigma_{12}\rho\eta_s$ is the signal absorption coefficient and $\alpha_p = L\sigma_{13}\rho\eta_p$ is the pump absorption coefficient. The fractional delay at the end of the fiber can be obtained from the phase shift at $z=L$, i.e., $F \equiv \phi(z=L)/(2\pi)$. As is seen in Eq. (13), the population oscillation of the unpaired ions and that corresponding to the paired ions are responsible for the signal delay.

3. MEASUREMENTS

The experimental setup is depicted in Fig. 2 and consists of a 1 m long EDF pumped with a 977 nm beam copropagating with a 1536 nm signal. The signal beam comes from a pigtailed distributed feedback (DFB) laser diode (Anritsu, GB5A016) operating at 1536 nm with a current and temperature controller (Thorlabs, ITC502) that allows us to keep the laser at room temperature. The signal beam is split into two beams: one part of the beam (1%) is sent directly to a switchable-gain amplified InGaAs photodetector (Thorlabs, PDA400) with 10 MHz bandwidth at the minimum gain setting, to be used as reference. The other part of the beam (99%) goes through an EDF and then to an identical photodetector. The EDF is pumped by a copropagating beam from a pigtailed DFB laser diode (Thorlabs, PL975P200) operating at 977 nm with a current and temperature controller (Thorlabs, ITC510). To

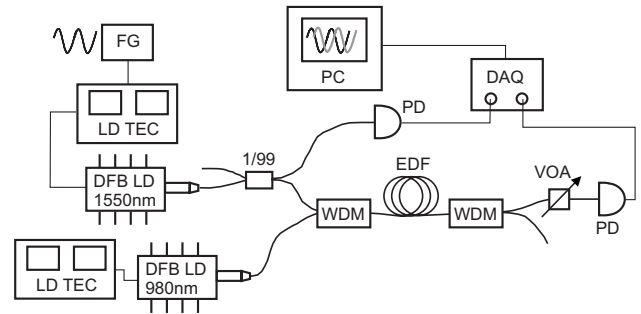


Fig. 2. Experimental setup used to measure slow and fast light in high-concentration EDFs. LD TEC: laser diode and temperature controller; FG: function generator; DFB LD: distributed feedback laser diode; WDM: wavelength division multiplexer; EDF: erbium-doped fiber; VOA: variable optical attenuator; PD: photodetector; DAQ: data acquisition card; PC: personal computer.

inject both signals into the EDF we use a wavelength division multiplexer WDM (Thorlabs, WD202A). Similarly, to separate the 977 nm signal from the signal that we want to analyze we use an identical WDM at the output of the EDF. Furthermore, an in-line variable optical attenuator (Thorlabs, VOA50) was placed in between the EDF and the detector to prevent saturation of the photodetector. Both the reference and the EDF signals are recorded with a fast data acquisition card (rate of 10 mega samples/s) (National Instruments, PCI-6115S Series) and then transferred to a computer for analysis. The experiment is controlled with a LABVIEW program.

The injection current of the laser signal was sinusoidally modulated by a function generator (Agilent, 33220A) so that the signal power injected into the fiber was $P = P_0 + P_m \cos(2\pi f_m t)$. We tested that the results reported here do not exhibit significant changes upon the change of the modulation amplitude. So we kept the ratio $P_m/P_0 = 0.5$ in all of the cases, being $P_0 = 0.5$ mW. We computed the time delay-advancement t_d from the correlation of the reference signal and the signal propagated through the EDF. The fractional delay-advancement is defined as $F = t_d/f_m$, i.e., the time delay normalized to the period of the modulated signal. With the aim of revealing the effect of ion pairs we consider two single mode Al_2SiO_5 -glass-based EDFs (provided by Liekii, Ltd.) with the same characteristics but with different ion concentrations: an EDF with moderate ion density $1.6 \times 10^{25} \text{ m}^{-3}$ (800 ppm), where interparticle interaction effects are expected to be negligible; and an ultrahighly doped erbium fiber with ion density $6.3 \times 10^{25} \text{ m}^{-3}$ (3150 ppm), where inhomogeneous upconversion processes are expected to occur. The fibers have a nominal mode field diameter at 1550 nm of $6.5 \mu\text{m}$, a fiber cladding of $245 \mu\text{m}$, and a numerical aperture of 0.2.

In the case of slow light based on CPO, there is an optimum modulation frequency (f_{opt}) where the fractional delay or advancement achieves its maximum value. This optimum modulation frequency corresponds to the half-width at half-maximum of the spectral hole induced by CPO effects in the absorption or gain spectrum and gives us an idea of the operating bandwidth of the system. Most practical applications require large fractional delays and large modulation bandwidths. The maximum fractional

advancement or delay is proportional to the unsaturated absorption coefficient of the erbium-doped medium α_s , i.e., to the ion concentration, which indicates that high doping levels lead to larger delays—advancements (see the analytical expressions deduced in [4,5]). The optimum frequency roughly follows the expression

$$f_{\text{opt}} \approx \frac{1}{2\pi\tau}(1 + \hat{P}_0 + \hat{P}_p) \equiv \frac{w_c}{2\pi\tau}. \quad (14)$$

Note that the operating bandwidth of the system does not change with ion density although it can be increased by means of the pump power, that is, the transparency spectral hole is power broadened.

A. Estimation of the Number of Ion Pairs

First of all, we have characterized the transmission of a continuous wave (CW) signal and pump through the fiber with moderate erbium dopant concentration (800 ppm) by measuring the corresponding output–input power curves. These curves were fitted by numerically solving the propagation equation of a CW signal [Eq. (11) without pump] and a CW pump [Eq. (12) without signal]. We considered that all the ions are isolated ($k=0$). Then, we obtain the following parameter values: $\sigma_{12}=\sigma_{21}=5.7$

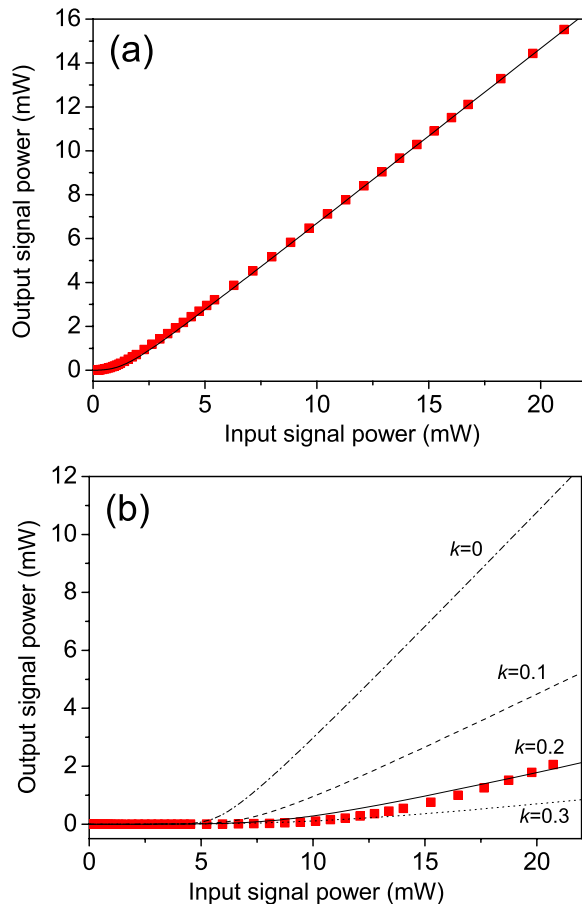


Fig. 3. (Color online) (a) Experimental (squares) and simulated (solid curve) signal output–input power curve for the moderate EDF. (b) Experimental (squares) signal output–input power curve for the ultrahighly EDF and the results of simulations with different fraction of ion pairs: $k=0$ (dashed-dotted curve), $k=0.1$ (dashed curve), $k=0.2$ (solid curve), and $k=0.3$ (dotted curve).

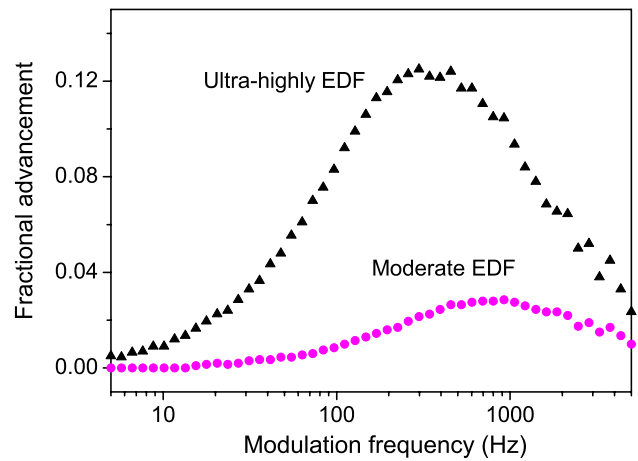


Fig. 4. (Color online) Fractional advancement F versus modulation frequency f_m for both fibers and a pump power of 108 mW.

$\times 10^{-25} \text{ m}^{-3}$, $\sigma_{13}=3 \times 10^{-25} \text{ m}^{-3}$, $A_s \approx 33 \mu\text{m}^2$ (signal mode field diameter $6.5 \mu\text{m}$), $A_p \approx 20 \mu\text{m}^2$ (pump mode field diameter $5.0 \mu\text{m}$), $A_c \approx 14 \mu\text{m}^2$ (fiber core diameter $4.2 \mu\text{m}$), and $\tau=10.5 \text{ ms}$, which are consistent with the values previously used in other works [4,12]. The insertion losses between the WDM coupler and the EDF were measured for the signal (0.8) and pump (0.65). The signal saturation power is $P_{\text{osat}} \approx 0.4 \text{ mW}$ and the pump saturation power is $P_{\text{psat}} \approx 1.3 \text{ mW}$. As an example, Fig. 3(a) shows the experimental and the simulated signal input–output power curves. In what follows we will use an average signal power of $P_0=0.5 \text{ mW}$, so $\hat{P}_0 \approx 1$.

To estimate the number of ion pairs in the ultrahighly EDF (3150 ppm) we measured the output–input power curve for a CW signal and compare it with the result of simulations [see Fig. 3(b)]. We developed simulations with different fraction of ion pairs that allowed us to see the PIQ effect in the propagation dynamics of the signal through the EDF. The PIQ strongly affects the slope effi-

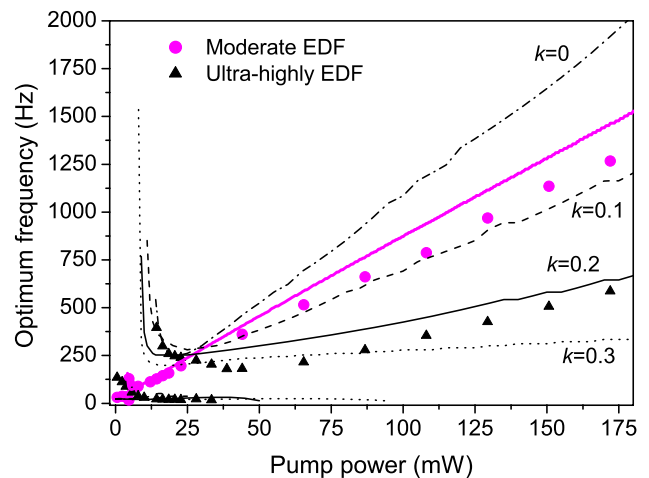


Fig. 5. (Color online) Experimental (circles) and simulated (thick curve) optimum frequency versus pump power for the moderate EDF. Experimental (triangles) optimum frequency versus pump power for the ultrahighly EDF and the results of simulations with different fractions of ion pairs: $k=0$ (dashed-dotted curve), $k=0.1$ (dashed curve), $k=0.2$ (solid black curve), and $k=0.3$ (dotted curve).

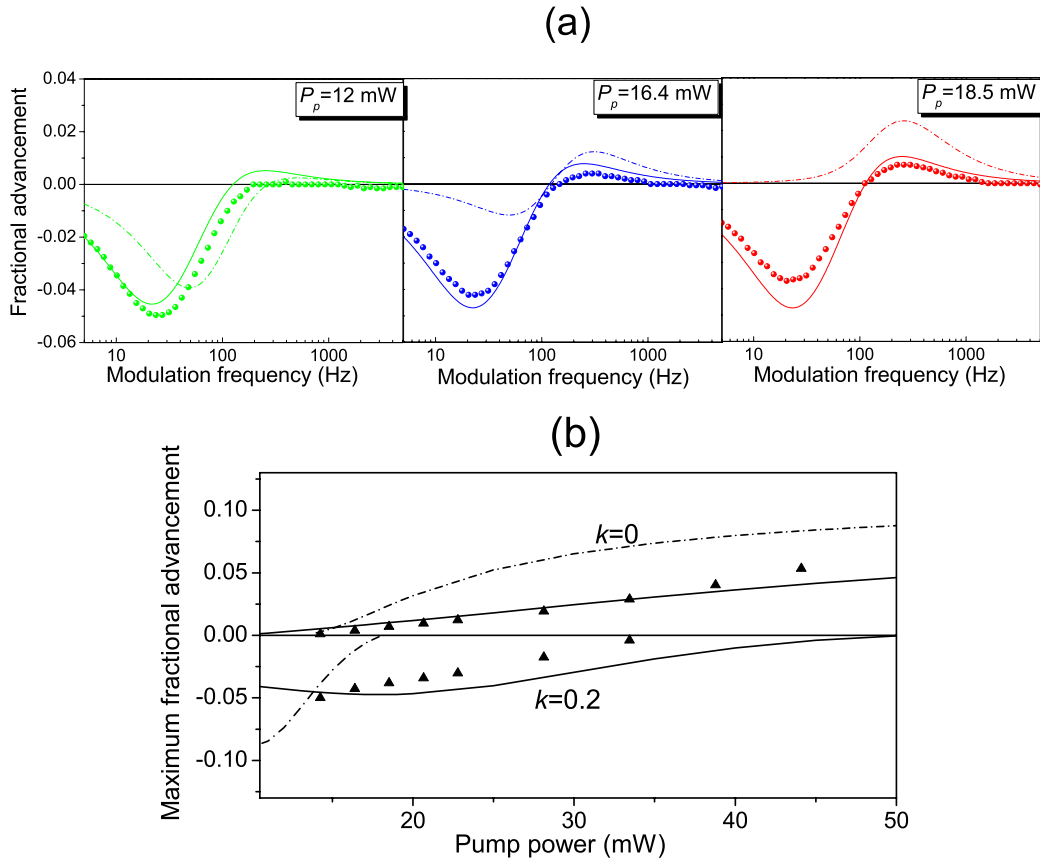


Fig. 6. (Color online) (a) Experimental (circles) fractional advancement F versus modulation frequency f_m for different pump powers. (b) Experimental (triangles) maximum fractional advancement–delay versus the pump power. Both figures correspond to the case of the ultrahighly EDF and the simulated curves have been done without PIQ (dashed-dotted curve) and with a fraction of ion pairs $k=0.2$ (solid curve).

ciency. These results suggested that there is 20% of ion pairs in the total ion concentration of this fiber.

B. Effect of Pair-Induced Quenching in the Slow- and Fast-Light Propagation

Let us analyze the effect of the PIQ in the fractional advancement F . First, we measure the variation of the fractional advancement F versus the modulation frequency f_m when pumping the fibers with an input pump power of 108 mW (see results in Fig. 4). Note that the maximum fractional advancement and the optimum modulation frequency at which this maximum occurs are very different for both fibers. We observe that fibers with a high doping level allow for larger advancements. For the moderate EDF the maximum fractional advancement achieved is around 0.03 whereas for the ultrahighly EDF the maximum fractional advancement increases by a factor of 4 (since its value is around 0.12). This increase factor is close to the ratio between the ion concentration of both fibers, as pointed out in our previous discussion. On the other hand, the optimum frequency shifts to smaller frequencies when increasing ion concentration. In particular, the frequency at which the maximum fractional advancement takes place appears around $f_{\text{opt}} \approx 790$ Hz for the moderate EDF, which is in agreement with Eq. (14). However, this value shifts to $f_{\text{opt}} \approx 350$ Hz for the ultrahighly EDF. Thus, the bandwidth of the system is hardly affected by the ion pairs present in this fiber.

To deeply analyze this point, let us see how the bandwidth changes with the pump power for both fibers. Figure 5 shows the optimum modulation frequency as a function of the pump power. At high pump powers the modulation frequency at which the maximum advancement is achieved increases linearly with pump power following Eq. (14) for the moderate EDF. For the ultrahighly EDF the slope of the curve of the optimum frequency with pump power deviates significantly from the theoretical prediction [Eq. (14)], which indicates that ion pairs degrade the bandwidth of the system. We have numerically solved Eqs. (11)–(13) for a fraction of ion pairs of 20% ($k=0.2$). The simulated value of the optimum frequency is plotted with a solid curve in Fig. 5. A good agreement with the experimental data is observed. Furthermore, in order to show the influence of ion pairs we also plotted in Fig. 5 the simulation results for different fractions of ions pairs. We observe that the slope of the optimum frequency versus pump power curve decreases as the fraction of ion pairs increases.

At moderate pump powers advancement or delay is achieved depending on the modulation frequency (see, for example, the value of the optimum frequencies obtained in the range of pump powers between 15 and 35 mW in the ultrahighly EDF shown in Fig. 5). This peculiar behavior has been reported in [16] and is due to the interplay between pump absorption and pump-power broadening of the spectral hole induced by coherent population

oscillations in these highly doped fibers. Thus, high-frequency modulated signals suffer strong advancement along the front part of the fiber and slightly delay along the last part of the fiber so a net advancement of these high-frequency signals is achieved. The opposite situation occurs for low frequency modulated signals, leading to a net delay [16]. As an example, we plot in Fig. 6(a) the fractional advancement–delay versus the modulation frequency for three different pump powers in the ultrahighly doped Er fiber. At 12 mW only delay is achieved for all the modulation frequencies, while at 18.5 mW advancement (delay) for high (low) frequency signals occurs so a transition from superluminal to subluminal propagation takes place solely by increasing the signal modulation frequency.

Let us analyze the effect of PIQ in this superluminal to subluminal transition. In Fig. 6(b) we plot the maximum fractional advancement–delay versus the pump power obtained for the ultrahighly EDF. We used a range of pump powers in which a transition from subluminal to superluminal propagation occurs. We developed simulations including the effect of a fraction of ion pairs of 20% (solid curve) and neglecting the PIQ effect (dashed-dotted curve). We conclude that ion pairs enlarge the transition region over a large range of pump powers. This enlargement can be also tested in detail in Fig. 6(a).

4. CONCLUSIONS

The effect of ion pairs in high-concentration erbium-doped fibers on slow- and fast-light propagation enabled by coherent population oscillations at room temperature has been experimentally investigated. We find that, although an increase of ion doping increases the fractional advancement obtained, the presence of erbium ion pairs in ultrahighly doped fibers degrades the bandwidth of the modulated signals that propagates at superluminal velocities. Furthermore, we observed that the enlargement of the range of pump powers at which a transition from subluminal to superluminal propagation takes place solely upon increasing the modulation frequency reported in ultrahighly doped fibers with respect to other less doped fibers is due to the presence of such ion pairs.

ACKNOWLEDGMENTS

This work has been supported by projects PR34/07-15847 Universidad Complutense de Madrid/Banco Santander Central Hispano, FIS2007-65382 Ministerio de Educación y Ciencia, and CCG07-UCM/ESP-2179 Universidad Complutense de Madrid-Comunidad de Madrid from Spain.

REFERENCES

1. K. Y. Song, M. G. Herráez, and L. Thèvenaz, "Observation of pulse delaying and advancement in optical fibers using stimulated Brillouin scattering," *Opt. Express* **13**, 82–88 (2005).
2. Y. Okawachi, M. S. Bigelow, J. E. Sharping, Z. Zhu, A. Schweinsberg, D. J. Gauthier, R. W. Boyd, and A. L. Gaeta, "Tunable all-optical delays via Brillouin slow light in an optical fiber," *Phys. Rev. Lett.* **94**, 153902 (2005).
3. J. E. Sharping, Y. Okawachi, and A. L. Gaeta, "Wide bandwidth slow light using a Raman fiber amplifier," *Opt. Express* **13**, 6092–6098 (2005).
4. A. Schweinsberg, N. N. Lepeshkin, M. S. Bigelow, R. W. Boyd, and S. Jarabo, "Observation of superluminal and slow light propagation in erbium-doped optical fiber," *Europhys. Lett.* **73**, 218–224 (2006).
5. M. S. Bigelow, N. N. Lepeshkin, and R. W. Boyd, "Observation of ultraslow light propagation in a ruby crystal at room temperature," *Phys. Rev. Lett.* **90**, 113903 (2003).
6. M. S. Bigelow, N. N. Lepeshkin, and R. W. Boyd, "Superluminal and slow light propagation in a room-temperature solid," *Science* **301**, 200–202 (2003).
7. L. W. Hillman, R. W. Boyd, J. Kransinski, and C. R. Stroud, "Observation of a spectral hole due to population oscillations in a homogeneously broadened optical absorption line," *Opt. Commun.* **45**, 416–419 (1983).
8. G. M. Gehring, A. Schweinsberg, C. Barsi, N. Kostinski, and R. W. Boyd, "Observation of backward pulse propagation through a medium with a negative group velocity," *Science* **312**, 895–897 (2006).
9. H. Shin, A. Schweinsberg, G. M. Gehring, K. Schwertz, H. J. Chang, R. W. Boyd, Q-H. Park, and D. J. Gauthier, "Reducing pulse distortion in fast-light pulse propagation through an erbium-doped fiber amplifier," *Opt. Lett.* **32**, 906–908 (2007).
10. F. Sanchez, P. L. Boudec, P.-L. Francois, and G. Stephan, "Effects of ion pairs on the dynamics of erbium-doped fiber lasers," *Phys. Rev. A* **48**, 2220–2229 (1993).
11. J. L. Wagener, P. F. Wysocki, M. J. F. Digonnet, H. J. Shaw, and D. J. DiGiovanni, "Effects of concentration and clusters in erbium-doped fiber lasers," *Opt. Lett.* **18**, 2014–2016 (1993).
12. P. F. Wysocki, J. L. Wagener, M. J. F. Digonnet, and H. J. Shaw, "Evidence and modelling of paired ions and other loss mechanisms in erbium-doped silica fibers," *Proc. SPIE* **1789**, 66–79 (1993).
13. J. Li, K. Duan, Y. Wang, W. Zhao, J. Zhu, Y. Guo, and X. Lin, "Modeling and effects of ion pairs in high-concentration erbium-doped fiber lasers," *J. Mod. Opt.* **55**, 447–458 (2008).
14. S. Melle, O. G. Calderón, F. Carreño, E. Cabrera, M. A. Antón, and S. Jarabo, "Effect of ion concentration on slow light propagation in highly doped erbium fibers," *Opt. Commun.* **279**, 53–63 (2007).
15. Y. Zhang, W. Qiu, J. Ye, N. Wang, J. Wang, H. Tian, and P. Yuan, "Controllable ultraslow light propagation in highly-doped erbium fiber," *Opt. Commun.* **281**, 2633–2637 (2008).
16. S. Melle, O. G. Calderón, C. E. Caro, E. Cabrera-Granado, M. A. Antón, and F. Carreño, "Modulation-frequency-controlled change from sub- to superluminal regime in highly doped erbium fibers," *Opt. Lett.* **33**, 827–829 (2008).
17. R. W. Boyd, D. J. Gauthier, and A. L. Gaeta, "Applications of slow light in telecommunications," *Opt. Photonics News* **17**, 18–23 (2006).